Journal of Materials Chemistry A

Accepted Manuscript

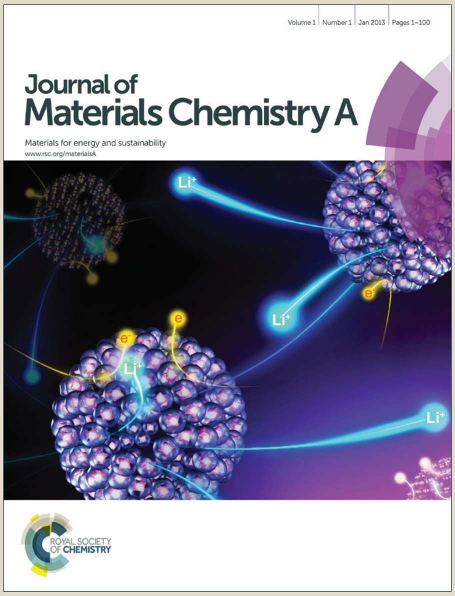

ROYAL SOCIETY OF CHEMISTRY

www.rsc.org/materialsA

Journal of Materials Chemistry A

RSCPublishing

COMMUNICATION

Cite this: DOI: 10.1039/x0xx00000x

Received 00th January 2013,
Accepted 00th January 2013

DOI: 10.1039/x0xx00000x

www.rsc.org/

Nitrogen-doped Open Pore Channeled Graphene Facilitating electrochemical Performance of TiO_2 nanoparticles as an Anode Material for Sodium Ion Batteries

Hyun Ae Cha,[a,d‡] Hyung Mo Jeong[b‡] and Jeung Ku Kang[a,b,c*]

We report that titanium dioxide nanoparticles anchored on nitrogen-doped open pore channeled graphenes exhibit high performance as anode materials for sodium ion batteries with a high reversible capacity of 405 mAh g^{-1} at a current density of 50 mA g^{-1}, excellent cycle stability with capacity of 250 mAh g^{-1} over 100 charge-discharge cycles at a current density of 100 mA g^{-1}, and superior rate capability. Also, it shows that high electrochemical performance is attributed to the facilitated ion diffusion by their open pore channels, in addition to the promoted electron transfer in electrochemical reactions by nitrogen-doping.

Sodium is an attractive candidate to satisfy the fast increasing demand of low-cost rechargeable batteries in the market.[1-6] However, the size of a sodium ion is about 55% larger than that for a lithium ion, thus requiring suitable host structures providing high storage capacity or facilitating its diffusion. However, there are very few reports suggested as anode structures for Na-ion batteries.[3-9] Nevertheless, they have relatively low capacity to realize the high performance as anode materials for Na-ion batteries.

Herein, we report high electrochemical performance of a TiO_2/nitrogen-doped open pore channeled graphene (TNCG) composite as an anode material for Na-ion batteries. The high electrical conductivity of the nitrogen-doped graphene is found to promote the electron transfer in electrochemical reaction. In addition, nitrogen doping has been found to be responsible for giving increased electrode/electrolyte wettability and ion absorption sites by generating extrinsic defects.[10-12] Moreover, open pore channels introduced into a two-dimensional porous graphene could lead to enhanced properties for capability in energy storage, which facilitate efficient access of electrolytes to the electrode and help for a fast diffusion by easier ionic transfer in regard to large size of sodium ions.[13-15] However, it should be noted that the graphene without open pore channels has a drawback that prevents its use in isolation as an anode material for batteries.[15, 16]

---

[a] Graduated School of Energy, Environment, Water, and Sustainability (EEWS), Korea Advanced Institute of Science and Technology (KAIST), 291 Daehak-ro, Yuseong-gu, Daejeon 305-701, Republic of Korea, E-mail: jeungku@kaist.ac.kr; Fax: +82-42-350-3310; Tel: +82-42-350-3378

[b] Department of Materials Science and Engineering, Korea Advanced Institute of Science and Technology (KAIST), 291 Daehak-ro, Yuseong-gu, Daejeon 305-701, Republic of Korea

[c] KAIST Institute Nano Century, Korea Advanced Institute of Science and Technology, 291 Daehak-ro, Yuseong-gu, Daejeon, 305-701, Republic of Korea

[d] Powder & Ceramic Division , Korea institute of Materials Science (KIMS) 797 Changwondaero, Seongsangu, Changwon, Gyeongnam, 642-831, Republic of Korea

‡ Hyun Ae Cha and Hyung Mo Jeong contributed equally to this work.

† Electronic Supplementary Information (ESI) available: See DOI: 10.1039/c000000x/

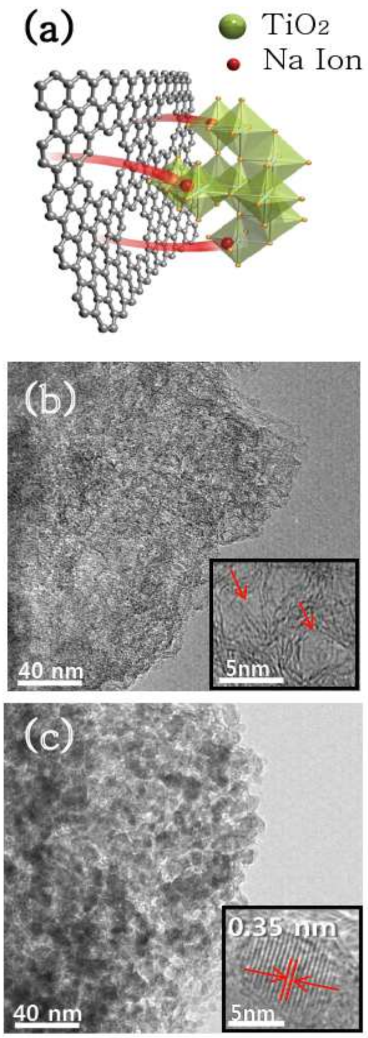

Fig. 1 (a) Schematic illustration of a sodium storage mechanism by the TiO_2/open pore channeled graphene composite, where the graphene, TiO_2 nanoparticles, and Na ions are in gray, green, and red colors, respectively. HRTEM image of (b) the CG and its inset showing open pore channels, and HR TEM image of (c) the TNCG and its inset showing the (101) lattice fringe.

Meanwhile, a TNCG electrode exhibits exceptional performance as an anode material for Na-ion batteries: a high capacity of 405 mAh g^{-1} obtained at a current density of 50 mA g^{-1}, excellent cycle stability retention over 100 charge-discharge cycles at a current density of 100 mA g^{-1}, and superior rate capability.

Figure 1a illustrates schematically behavior for a sodium storage mechanism in the synthesized TNCG. In the charge-discharge process, open pores in the channeled graphene facilitate easier transfer of sodium ions to each inter-layered graphene sheet with increased ion diffusivity. Figure 1b and c also show the transmission electron microscopy (TEM) images of following samples; the open channeled graphene (CG) with ca. 5 nm size pores synthesized by the microwave synthesis (Figure 1b). Then, the nitrogen-doped open channeled graphene (NCG) was prepared via chemical vapor deposition (CVD) process using the CG. Next, the TNCG was synthesized by the hydrothermal synthesis (130^{o}C, 2 h) using TiO_2 precursors and NCG (Figure 1c). The architecture of the TNCG is found to have 5~8 nm TiO_2 nanoparticles well dispersed on the NCG.

Moreover, we find that all the identified x-ray diffraction (XRD) peaks are in accordance with those for the anatase TiO_2 (JCPDS card no. 21-1272), as demonstrated in Figure 2a. This implies the complete formation of the anatase TiO_2 during the hydrothermal process. Furthermore, the Raman analysis of Figure 2b supports that the TNCG is composed of TiO_2 nanoparticles and the NCG. The pore size distribution of the TNCG was obtained from a micropore plot using the NLDFT method (Figure 2c). As can be seen from the plot, the TNCG has pores of 24 nm and 5 nm sizes while the TiO_2/nitrogen-doped graphene displays pores of only about 25 nm size (Figure S4c). The pores of 5 nm size corresponds to the sizes for ion channels in the TNCG, synthesized using oxidation-etching. Furthermore, to analyze the chemical binding states of the as-prepared sample, an X-ray photoelectron spectroscopy (XPS) analysis was carried out and the results were provided in Figure 2d. These indicate that there are three different types for nitrogen configurations[17-20] including pyridinic N (N-6, 401.6), pyrrolic N (N-5, 400.2), and quaternary N (N-Q, 398.6) states in the TNCG.

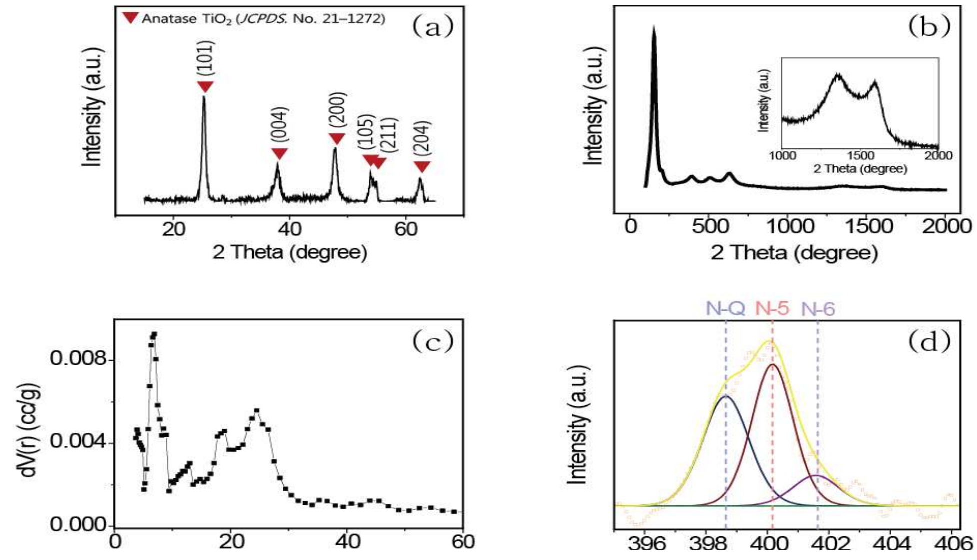

Fig.2 (a) XRD patterns, (b) Raman spectra with an excitation laser wavelength 514 nm, (c) BET pore distribution peaks, and (d) XPS N s1 spectra of the TNCG.

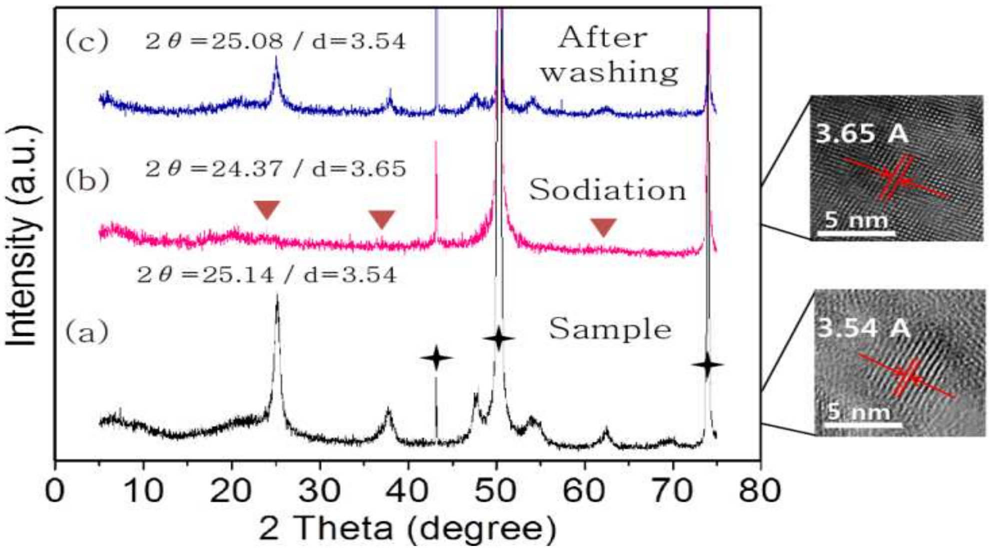

Fig. 3 (a) XRD patterns for the TNCG samples before and after sodiation and after washing out; ✦ indicates the peak from the Cu foil used to the current collector for the anode electrode, ▼shows the peak shifting of the TNCG. HRTEM images of the TNCG as an anode electrode for the sodium ion battery, (b) before and (c) after discharging. When discharged to 0.01 V (vs Na/Na$^+$) after cycling, the half-cell was disassembled to obtain the electrode film. The corresponding FFT are shown in the inset.

Figure 3 shows the effect of sodiation in a synthesized TNCG. The structural analysis and its electrochemical performance support that the anatase TiO_2 gives sites to store sodium ions and that the intercalation mechanism is dominant in the electrochemical sodium ion insertion/desertion process. Figure 3a, b and c shows the XRD patterns for the samples before sodiation, after sodiation, and after desodiation by the washing treatment, respectively. When the electrode is discharged to 0.01 V (vs Na/Na$^+$) after cycling, the half-cell was disassembled to obtain the sodiated electrode film in the Ar-filled glove box for ex-situ diffraction measurements. It is observed that the sodium ion insertion affects the structure of the TNCG. There is a slight shift of the peak position especially at the (101) plain (2θ = 25.14 degrees), as seen in Figure 3b. After washing with deionized water (DIW), the sodium is desodiated and it is found that the XRD pattern is the same as that for the original TNCG (Figure 3c). In Figure S1, the white color of the anatase TiO_2 was changed into the black color due to formation of a new phase obtained at a 0.01 V (Na/Na$^+$) after discharging, resulting in reduction of Ti^{4+} to Ti^{3+}.[21,22] In addition, the black color is changed into the white color as Ti^{3+} returns to Ti^{4+} by washing out sodium ions. These results clearly elucidate that the anatase TiO_2 of the TNCG can store sodium ions. The insets in the Figure 3a and b shows the high-resolution TEM (HRTEM) images of the anatase TiO_2 with (101) lattice fringes. When sodium ions were inserted into TiO_2, the interlayer spacing of the (101) plane was increased to 0.365 nm from 0.354 nm. This implies that a volume expansion occurs after insertion of sodium ions into TiO_2. It is consistent with the XRD patterns of Figure 3a and b.

The electrochemical performance of the electrode was also evaluated by using a half-cell combined with a sodium metal electrode. Figure 4a shows the representative cyclic voltammetry (CV) curves of the TNCG electrode in a range of 0.01 and 3 V at a scan rate of 0.1 mV s^{-1}. The CV curve of the TNCG has a combined shape of the NCG and bare TiO_2 (BTO) curves (Figure S6a, b). This indicates that sodium ions are stored in both the TiO_2 and also the graphene. In Figure 4b, the capacity of TNCG (405 mAh g^{-1}) is about 4 times higher than that of TiO2/graphene composite (105 mAh g^{-1}) because the open pore channels facilitate easier transfer of sodium ions to each inter-layered graphene sheet. Figure 4c shows that the rate performance of the TNCG is substantially superior to that of the TiO_2/graphene composite as the cycles are increased to high current densities of 1000 mA g^{-1} from 50 mA g^{-1}. The graph of the TiO_2 combined with the graphene without open pore channels reveals excellent cycling performance but with low capacity. For example, the specific capacity of the TNCG at a rate of 50 mA g^{-1} is about 405 mAh g^{-1}, which is almost 3 times higher than that of TiO_2 nanoparticles combined with the graphene without open pore channels (135 mAh g^{-1}). Also, the TNCG has a very high specific capacity (140 mAh g^{-1}) even at the highest rate of 1000 mA g^{-1}, where discharge takes only 6 min, which is considered to be due to the fast transfer of sodium ions via open channels of the graphene. It should be noted that this is on exceptionally high capacities compared with other results on titanate materials.[23, 24] Moreover, we find that the specific capacity of the TNCG at 50 mA g^{-1} recovers to the initial value, owing to its high reversibility. The cycling behavior for the TNCG electrode at a current density of 100 mA g^{-1} is also shown in Figure 4d. After 100 cycles, the capacity of the TNCG was still well retained with high capacity: 250.78 mAh g^{-1} after 100 cycles at a current density of 100 mA g^{-1}. Consequently, these results demonstrate that the TNCG delivers a high reversible sodium storage capacity compared with previously reported anode materials of Na-ion batteries,[9, 23-25] as described and compared in more details by the supplementary information (Fig. S7). According to the electrochemical performances, the open pore channels on graphene provide the easy access to the sodium ions and the electrolyte during the cell operation. In addition, on comparison of electrochemical impedance spectra (EIS) for pristine G and CG (see Supplementary Fig. S8), the radius for the semicircles of the CG electrode in the

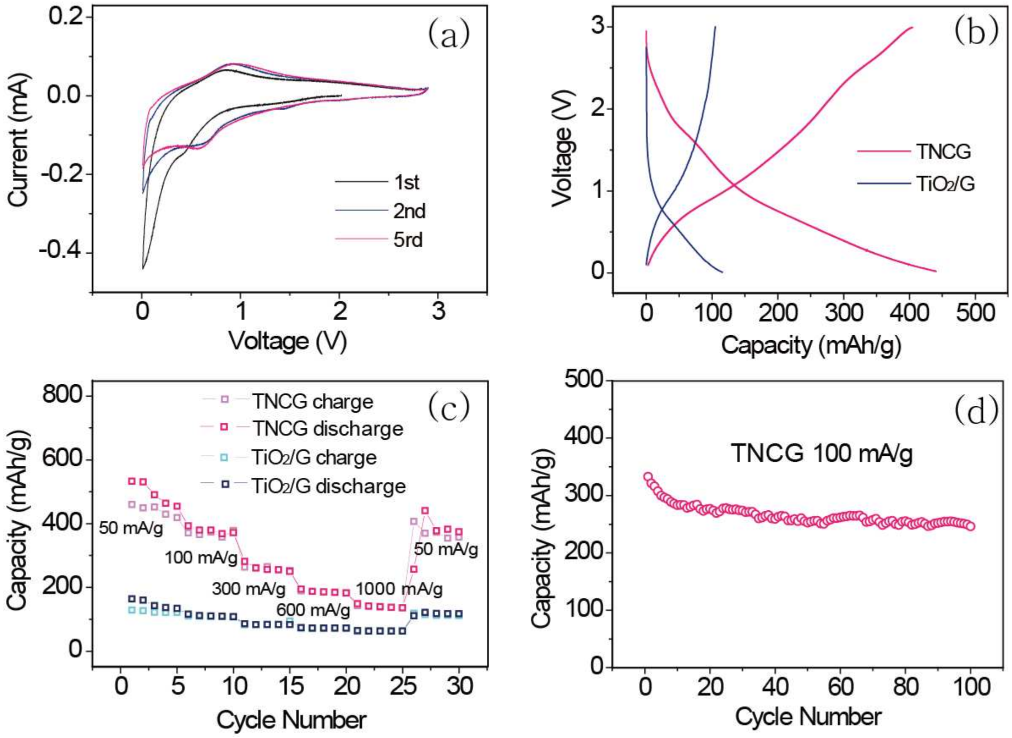

Fig. 4 (a) The initial three CV of the TNCG electrode at a scan rate of 0.1 mV s^{-1}. (b) Cyclic performance of BTO and TNCG electrodes, respectively, at a current rate of 100 mA g^{-1}. (c) The galvanostatic charge-discharge curve of the TNCG and TiO_2/graphene composite at a current rate of 50 mA g^{-1}. (d) Rate capability of the TNCG and TiO_2/graphene composite electrodes at various current rates from 50 mA g^{-1} to 1000 mA g^{-1}.

high-medium frequency region is smaller than that of the G electrode, suggesting that the charge-transfer resistance of the CG is lower than that of the G electrode. This verifies that the open channeled on graphene sheets improve the ion accessibility and conductivity of the overall electrode. In addition, the electrochemical impedance spectroscopy (EIS) curves of BTO and TNCG samples, as seen in Figures S9, show that the radius of the semicircles of the TNCG electrode in the high-medium frequency region is smaller than that of the BTO electrode, suggesting that the charge-transfer resistance of the TNCG is much lower than that of the BTO electrode. Even the TCG electrode with the open channeled graphene is found to show the semi-circle EIS curve having a much larger radius than that of the TNCG electrode. This supports that the nitrogen-doped graphene sheets improve the conductivity of the overall electrode. Furthermore, the electrochemical measurements support hat the TNCG shows quite stable cycle performance compared with those for other materials of Na-ion batteries.[23-27]

Moreover, the supplementary information of Figure S10 shows the cycle performance of graphene (G) and NCG samples. The results show that the NCG has more stable cycle performance than the graphene without open pore channels at a current density of 25 m A g^{-1}. This supports that the pores in the graphene serve as open channels facilitating an each movement of Na ions while nitrogen-doping gives a better conductivity than that of the pristine graphene without nitrogen-doping. In addition, to explore the possibility for our anode electrodes to be used as practical devices, we have performed additional experiments (Fig. S11). It is determined that the anode hybrid fabricated on TiO_2 nanoparticles and the nitrogen-doped open pore channeled graphene has high capacity even at a potential of 2.5 V. Consequently, these results show that open channels and nitrogen-doping of the graphene are responsible for the facilitated transfer of sodium ions and the increased electron transfer, thus demonstrating high electrochemical performance for active TiO_2 nanoparticles as anode materials for sodium ion batteries.

Conclusions

In summary, we have demonstrated high electrochemical performance of the TNCG as an anode material for Na-ion batteries. The synthesized composites showed i) the outstanding specific capacities at high current densities, ii) the stable cycling performance of capacity during sodium - ion insertion / desertion especially at high current densities; and iii) the good rate reversibility at a current density of 50 ~ 1000 mA g^{-1}. This demonstrates that open pore channels especially efficient for large size sodium ions and nitrogen-doping of the NCG are very important for increased capacity of TiO_2 nanoparticles by enabling improved ionic and electronic transfers, thus implying that the NCG could be employed to realize high performance with high capacity and stable cycling properties on combination of active other anode nanoparticles for Na-ion batteries.

Acknowledgements

This research was supported by the Secondary Battery Program (2010-0029042) and the National Research Foundation grants (2012-0001174). Also, it was supported by the Priority Research Centers Program (2011-0031407), the Global Frontier R&D Program (2013-073298) on Center for Hybrid Interface Materials (HIM) funded by the Ministry of Science, ICT & Future Planning. In addition, H.A. Cha and H. M. Jeong were supported by the National Research Foundation of Korea (NRF) grant funded by the Ministry of Science, ICT & Future Planning (2011-0028737) and the Korea Center for Artificial Photosynthesis (KCAP) located in Sogang University(2009-0093881).

Notes and references

1. J.-M. Tarascon and M. Armand, *Nature*, 2001, **414**, 359-367.
2. J. B. Goodenough and Y. Kim, *Chem Mater*, 2009, **22**, 587-603.
3. V. Chevrier and G. Ceder, *J Electrochem Soc*, 2011, **158**, A1011-A1014.
4. S. P. Ong, V. L. Chevrier, G. Hautier, A. Jain, C. Moore, S. Kim, X. Ma and G. Ceder, *Energ Environ Sci*, 2011, **4**, 3680-3688.
5. V. Palomares, P. Serras, I. Villaluenga, K. B. Hueso, J. Carretero-González and T. Rojo, *Energ Environ Sci*, 2012, **5**, 5884-5901.
6. D. A. Stevens and J. R. Dahn, *J Electrochem Soc*, 2000, **147**, 1271-1273.
7. M. D. Slater, D. Kim, E. Lee and C. S. Johnson, *Adv Funct Mater*, 2013, **23**, 947-958.
8. V. Palomares, M. Casas-Cabanas, E. Castillo-Martínez, M. H. Han and T. Rojo, *Energy Environ. Sci.*, 2013.
9. H. Xiong, M. D. Slater, M. Balasubramanian, C. S. Johnson and T. Rajh, *J Phys Chem Lett*, 2011, **2**, 2560-2565.
10. H. M. Jeong, S. Y. Lee, W. H. Shin, J. H. Kwon, A. Shakoor, T. H. Hwang, S. Y. Kim, B. S. Kong, J. S. Seo, Y. M. Lee, J. K. Kang and J. W. Choi, *Rsc Adv*, 2012, **2**, 4311-4317.
11. D. D. Cai, D. D. Li, S. Q. Wang, X. F. Zhu, W. S. Yang, S. Q. Zhang and H. H. Wang, *J Alloy Compd*, 2013, **561**, 54-58.
12. Z. H. Wang, L. Qie, L. X. Yuan, W. X. Zhang, X. L. Hu and Y. H. Huang, *Carbon*, 2013, **55**, 328-334.
13. Z. J. Fan, Q. K. Zhao, T. Y. Li, J. Yan, Y. M. Ren, J. Feng and T. Wei, *Carbon*, 2012, **50**, 1699-1703.
14. Y. W. Zhu, S. Murali, M. D. Stoller, K. J. Ganesh, W. W. Cai, P. J. Ferreira, A. Pirkle, R. M. Wallace, K. A. Cychosz, M. Thommes, D. Su, E. A. Stach and R. S. Ruoff, *Science*, 2011, **332**, 1537-1541.
15. H. G. Wang, Z. Wu, F. L. Meng, D. L. Ma, X. L. Huang, L. M. Wang and X. B. Zhang, *Chemsuschem*, 2013, **6**, 56-60.
16. P. Lian, X. Zhu, S. Liang, Z. Li, W. Yang and H. Wang, *Electrochim Acta*, 2010, **55**, 3909-3914.
17. H. B. Wang, T. Maiyalagan and X. Wang, *Acs Catal*, 2012, **2**, 781-794.
18. D. C. Wei, Y. Q. Liu, Y. Wang, H. L. Zhang, L. P. Huang and G. Yu, *Nano Lett*, 2009, **9**, 1752-1758.
19. C. Burda, Y. B. Lou, X. B. Chen, A. C. S. Samia, J. Stout and J. L. Gole, *Nano Lett*, 2003, **3**, 1049-1051.
20. H. M. Jeong, J. W. Lee, W. H. Shin, Y. J. Choi, H. J. Shin, J. K. Kang and J. W. Choi, *Nano Lett*, 2011, **11**, 2472-2477.
21. A. R. Armstrong, G. Armstrong, J. Canales, R. García and P. G. Bruce, *Adv Mater*, 2005, **17**, 862-865.
22. M.-S. Song, A. Benayad, Y.-M. Choi and K.-S. Park, *Chem. Commun.*, 2011, **48**, 516-518.
23. A. Rudola, K. Saravanan, C. W. Mason and P. Balaya, *J Mater Chem A*, 2013, **1**, 2653-2662.
24. Y. Sun, L. Zhao, H. Pan, X. Lu, L. Gu, Y.-S. Hu, H. Li, M. Armand, Y. Ikuhara and L. Chen, *Nature communications*, 2013, **4**, 1870.
25. D. W. Su, H. J. Ahn and G. X. Wang, *Chem Commun*, 2013, **49**, 3131-3133.
26. W. Wang, C. J. Yu, Y. J. Liu, J. G. Hou, H. M. Zhu and S. Q. Jiao, *Rsc Adv*, 2013, **3**, 1041-1044.
27. W. Wang, C. J. Yu, Z. S. Lin, J. G. Hou, H. M. Zhu and S. Q. Jiao, *Nanoscale*, 2013, **5**, 594-599.

We report electrochemical performance of a TiO_2 combined with a nitrogen-doped open channeled graphene anode composite for sodium ion batteries.